

Amplitude-based optimal respiratory gating in positron emission tomography in patients with primary lung cancer

Willem Grootjans · Lioe-Fee de Geus-Oei ·
Antoi P. W. Meeuwis · Charlotte S. van der Vos ·
Martin Gotthardt · Wim J. G. Oyen · Eric P. Visser

Received: 11 March 2014 / Revised: 28 May 2014 / Accepted: 18 July 2014 / Published online: 6 August 2014
© European Society of Radiology 2014

Abstract

Objectives Respiratory motion during PET imaging introduces quantitative and diagnostic inaccuracies, which may result in non-optimal patient management. This study investigated the effects of respiratory gating on image quantification using an amplitude-based optimal respiratory gating (ORG) algorithm.

Methods Whole body FDG-PET/CT was performed in 66 lung cancer patients. The respiratory signal was obtained using a pressure sensor integrated in an elastic belt placed around the patient's thorax. ORG images were reconstructed with 50 %, 35 %, and 20 % of acquired PET data (duty cycle). Lesions were grouped into anatomical locations. Differences in lesion volume between ORG and non-gated images, and mean FDG-uptake (SUV_{mean}) were calculated.

Results Lesions in the middle and lower lobes demonstrated a significant SUV_{mean} increase for all duty cycles and volume decrease for duty cycles of 35 % and 20 %. Significant increase in SUV_{mean} and decrease in volume for lesions in the upper lobes were observed for a 20 % duty cycle. The SUV_{mean} increase for central lesions was significant for all duty cycles, whereas a significant volume decrease was observed for a duty cycle of 20 %.

Conclusions This study implies that ORG could influence clinical PET imaging with respect to response monitoring and radiotherapy planning.

Key Points

- Quantifying lesion volume and uptake in PET is important for patient management
- Respiratory motion artefacts introduce inaccuracies in quantification of PET images
- Amplitude-based optimal respiratory gating maintains image quality through selection of duty cycle
- The effect of respiratory gating on lesion quantification depends on anatomical location

Keywords Respiratory gating · Standardized uptake value · ^{18}F -FDG · PET/CT · Lung cancer

Introduction

Positron Emission Tomography (PET) in combination with X-ray computed tomography (CT) is an essential multimodality molecular imaging platform for accurate staging and diagnosis of a variety of diseases, particularly in oncology [4, 15]. The advantage of PET/CT imaging is that it permits the acquisition of both anatomical and functional images of the patient; improving detection, localization and characterization of disease sites [4, 26]. In addition, quantitative indices in PET, such as the standardized uptake value (SUV) [2] and total lesion glycolysis (TLG) [8, 28], can be used to provide important prognostic information. Furthermore, it has been established that molecular imaging with PET is valuable in the early assessment and prediction of therapy response of several cancers [10–12, 21].

However, due to the relatively long image acquisition times, typically 3–4 minutes for a single bed position, patients are instructed to breathe freely during PET imaging. As a consequence, motion artefacts due to the respiratory cycle can result in significant blurring of structures within the thorax

W. Grootjans (✉) · L.-F. de Geus-Oei · A. P. W. Meeuwis ·
C. S. van der Vos · M. Gotthardt · W. J. G. Oyen · E. P. Visser
Department of Radiology and Nuclear Medicine, Radboud
University Medical Center, P.O. Box 9101, 6500 HB Nijmegen,
The Netherlands
e-mail: willem.grootjans@radboudumc.nl

L.-F. de Geus-Oei
MIRA Institute for Biomedical Technology and Technical Medicine,
University of Twente, Enschede, The Netherlands

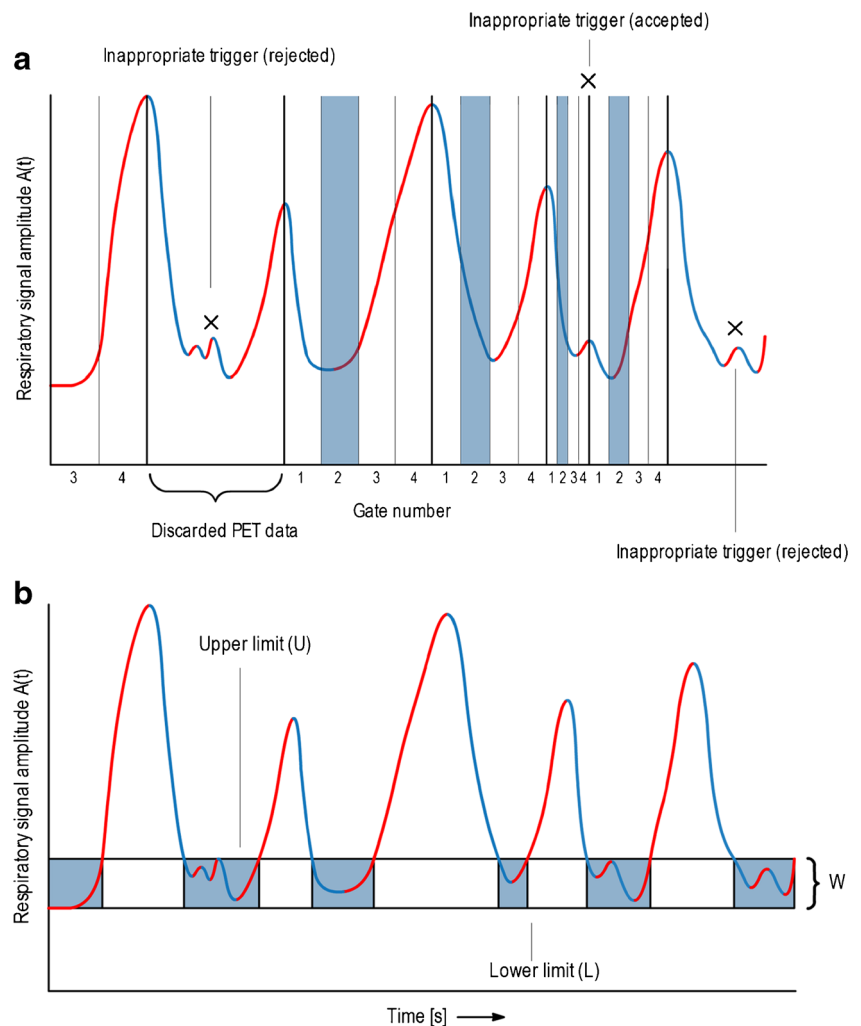
and upper abdomen, resulting in underestimation of lesion radiotracer uptake and overestimation of lesion volume in PET images [5, 7, 13]. If uncorrected, these artefacts can introduce diagnostic uncertainties, inaccuracies in definition of target volumes for radiation treatment planning, and hinder adequate monitoring of therapy response

Different respiratory gating approaches have been developed in order to correct PET images for respiratory motion artefacts, relying on the selection of data in specific time intervals within the respiratory cycle, thereby creating an image in which the main respiratory motion components are removed. This is usually accomplished by simultaneously recording a surrogate signal correlated with the patient’s respiratory cycle with the PET data [19, 22]. Using the surrogate signal acquired, PET data can be selected by means of dividing each respiratory cycle into a fixed number of gates (phase-based gating) or by defining a certain amplitude range (amplitude-based gating) [7, 9, 18], as depicted in Fig. 1.

However, difficulties in retrospective gating approaches are related to the maintenance of acceptable

image quality in the presence of irregular breathing frequencies. Particularly in phase-based respiratory gating approaches, discarded PET data due to rejection of inappropriate triggers results in reduction of image quality whilst acceptance of inappropriate triggers results in the definition of gates in different phases of the respiratory cycle, as depicted in Fig. 1a. In this study, the effects of respiratory gating in modern high resolution PET imaging on quantification of lesion volume and FDG-uptake for lesions in the thorax were investigated using an amplitude-based optimal respiratory gating (ORG) algorithm. In contrast to many other respiratory gating algorithms, ORG safeguards image quality through calculation of an optimal amplitude range for a specified percentage of acquired PET data. The performance of ORG in a clinical whole body imaging protocol was evaluated in a large representative group of patients with primary lung cancer. In particular, the effect of lesion anatomical location and different inputs for the algorithm were investigated.

Fig. 1 Phase-based and amplitude-based gating approaches for PET. **a** Phase-based gating **b** Amplitude-based gating. In phase-based gating, each respiratory cycle is divided in a fixed number of gates (in this case, four) and data acquired in a specific gate is used for image reconstruction. Amplitude-based gating relies on definition of an upper and lower amplitude limit. PET data acquired when the amplitude of the respiratory signal falls in the defined amplitude range will be used for image reconstruction. In case of the ORG algorithm, an optimal amplitude range is defined according to the specified amount of data that needs to be used for image reconstruction (total sum of the areas shaded in blue)



Materials and methods

Patients

This study was approved by the institutional review board (IRB) of the Radboud university medical center. A total of 66 patients from our fast-track outpatient diagnostic program with histologically confirmed primary lung cancer were included in this study. Patient characteristics are summarized in Table 1.

Image acquisition

Whole body FDG-PET imaging was performed using a Biograph 40 mCT (Siemens Medical Solutions, Knoxville Tennessee, USA) PET/CT. The PET system has an extended axial field of view (FOV) of 216 mm with four lutetium oxyorthosilicate (LSO) detector rings (TrueV). The amount of

administered FDG was adjusted to the patient's weight (3.2 ± 0.2 MBq/kg). Respiratory gating was performed on bed positions covering the thorax and upper abdomen. Gated and non-gated bed positions were acquired during patient free breathing for six minutes and two minutes, respectively. The respiratory signal was obtained using an Anzai AZ-733 V respiratory gating system (Anzai Medical Co. Ltd., Tokyo, Japan). This system consists of a pressure sensor integrated in an elastic belt, which is placed around the patient's thorax. A whole body low dose (LD) CT was acquired during free-breathing for the purpose of attenuation correction and anatomical reference. The X-ray tube peak voltage (kVp) was set to 100 kV and 120 kV for patients with body mass <70 kg and >70 kg, respectively. Appropriate conversion of CT images acquired using different kVps to 511 keV annihilation photon attenuation maps was performed using a kVp-dependent transformation, as implemented in the Siemens mCT software [6]. The X-ray tube current was modulated using CARE Dose4D, with a reference tube current of 50 mAs.

Table 1 Characteristics of the patient population used for this study

Characteristics of patient population	
Male(Female)	44(22)
Median age (range) [y]	66 (33-85)
Body mass [†] [kg]	78±15
Administered FDG activity ^a [MBq]	253±49
Histological type	
Small cell lung cancer	6
Non-small cell lung cancer	60 ^b
Squamous cell carcinoma	29
Adenocarcinoma	26
Large cell carcinoma	1
Bronchioloalveolar carcinoma	2
Adenosquamous carcinoma	1
Disease stage ^c	
Ia	5
Ib	7
IIa	8
IIb	0
IIIa	13
IIIb	14
IV	19

^a Data are reported as mean±standard deviation

^b Histology confirmed the presence of a NSCLC lesion in one patient. However, further immunohistological differentiation was not possible due to the quality of the obtained histological specimen and additional invasive diagnostic procedures were waived due to severe morbidity of the patient

^c Disease stage at the time of the gated PET acquisition

FDG=¹⁸F-Fluorodeoxyglucose

NSCLC=Non-small cell lung cancer

PET=Positron emission tomography

Respiratory gating

Respiratory gating was performed on the list-mode data with an amplitude-based ORG algorithm, integrated in the Syngo 2011A MI.PET/CT software, designated HD·Chest by Siemens. The main user input for the ORG algorithm is the percentage duty cycle, which is the percentage of the total acquired true coincidences used for image reconstruction. The ORG algorithm calculates an optimal amplitude range for a given duty cycle [13]. The algorithm starts by calculating the amplitude range for different values of the lower limit (L). With each value of L, the upper limit (U) is adjusted to include the specified percentage of the acquired PET data, and an amplitude range (W) is calculated through a simple subtraction (U-L). The optimal amplitude range is defined as the smallest amplitude range obtained and calculated by minimizing W, as depicted in Fig. 1b.

Selection of the percentage duty cycle permits the user to control the amount of noise versus the residual motion components in the reconstructed images. In this study, ORG images were reconstructed using duty cycles of 20 %, 35 %, and 50 %, corresponding with 72 seconds, 126 seconds and 180 seconds of PET data, respectively. For the non-gated images, the first 126 seconds of the acquired data were used for image reconstruction, resulting in an equal amount of acquired true coincidences as the ORG images reconstructed with a duty cycle of 35 %.

Image reconstruction

The CT images used for attenuation correction were reconstructed with a B19f convolution kernel and a slice thickness of 5.0 mm, whereas CT images used for the purpose of

anatomical reference were reconstructed with a B31f convolution kernel and a slice thickness of 3.0 mm. The PET images were reconstructed with the TrueX algorithm (with a spatially varying point spread function (PSF)) and the incorporation of time-of-flight (TOF) measurements (Ultra-HD PET). Image reconstruction was performed with three iterations, 21 subsets, and a matrix size of 400×400 (pixel spacing of 2.04 mm). The slice thickness of the PET images was matched to the slice thickness of the attenuation CT and post reconstruction filtering was performed with a 3D Gaussian filter kernel with a full width at half maximum (FWHM) of 3.0 mm.

Image analysis

Analysis of the FDG PET images was performed using the Inveon Research Workplace 4.1 Software (Preclinical Solutions, Siemens Medical Solutions USA, Knoxville Tennessee, USA). Lesions were delineated using a region growing segmentation algorithm with a segmentation threshold at 40 % of SUV_{max} [14]. Differences in lesion volume between non-gated and ORG images, as determined by the 40 % SUV_{max} isocontour, and in mean FDG-uptake of the corresponding volumes (SUV_{mean}) were calculated. In addition, noise characteristics were determined by placing a volume of interest (VOI) in the parenchyma of the contralateral lung and recording the mean and standard deviation of the SUV voxel values within these volumes. Image noise was expressed by the coefficient of variation, defined as the ratio of the standard deviation to the mean.

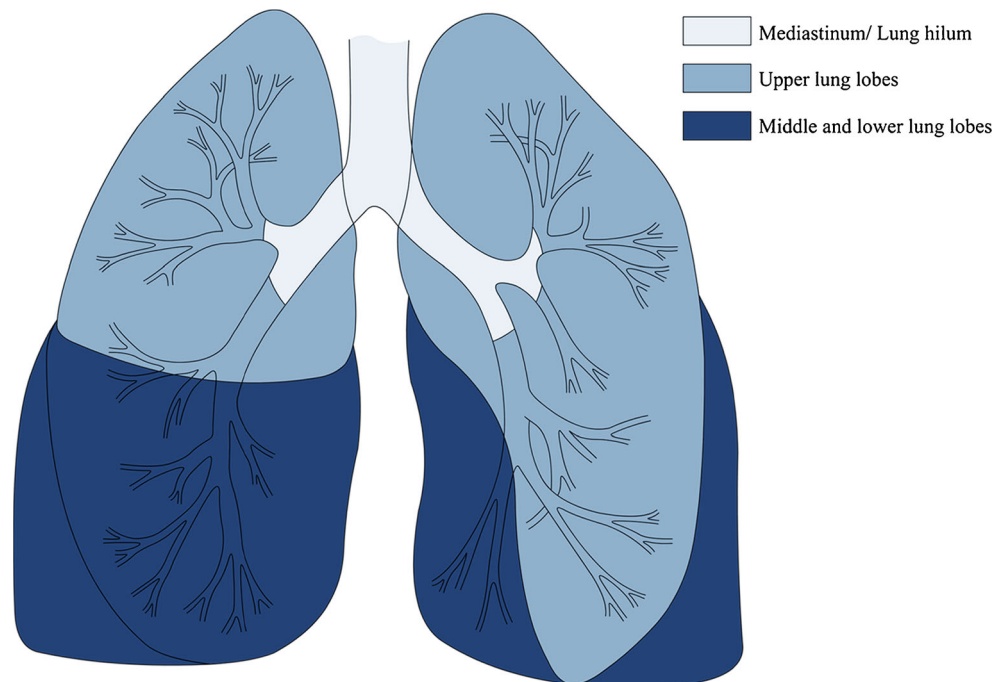
Lesion localization

It has been well established that the nature and magnitude of the motion of structures within the thorax are dependent on anatomical location [19]. Therefore, it is expected that the effects of respiratory gating also demonstrate such an anatomical dependency. In order to determine the effect of anatomical location on the quantification of lesion volume and FDG-uptake, lesions were grouped according to their anatomical location within the lungs. These locations are the 1) mediastinum/lung hilum (central group), 2) middle and lower lobes, 3) and upper lobes. Lesions which demonstrate invasive growth into or attachment to large structures (i.e., the main bronchi, arteries and veins) of the lung hilum or mediastinum, are assigned to the central group. The anatomical groups defined for this study are depicted in Fig. 2.

Statistics

Statistical analysis was performed using the Wilcoxon signed-rank test for paired variables using SPSS Statistics 20 (IBM, Chicago Illinois, USA) and statistical significance was defined for $p < 0.05$. Lesion volume and SUV_{mean} in the ORG images reconstructed with different duty cycles were compared with the non-gated images of the same patient. A Bonferroni correction was performed to correct for multiple testing through multiplication of the p -value with the number of statistical tests (in this case, six). Reported p -values have been Bonferroni corrected unless otherwise stated.

Fig. 2 Schematic representation of the three anatomical groups defined.



Results

Lesions in the ORG images demonstrated a statistically significant increase in SUV_{mean} values when compared to the non-gated images. The SUV_{mean} increase was $6.2 \pm 12.2\%$ ($p < 0.0001$), $7.4 \pm 13.3\%$ ($p < 0.0001$), and $9.2 \pm 14.0\%$ ($p < 0.0001$), for duty cycles of 50 %, 35 % and 20 %, respectively. Furthermore, a concomitant decrease in lesion volume of $6.9 \pm 19.6\%$ ($p = 0.02$), $8.5 \pm 19.3\%$ ($p < 0.0001$), and $11.3 \pm 20.2\%$ ($p < 0.0001$) was observed. The mean volume of the lesions, as determined on the non-gated images, was 18.7 ± 33.9 mL (range 0.37–230 mL). The absolute SUV_{mean} value of the lesions on non-gated images was 10.7 ± 6.3 $g \cdot mL^{-1}$. In ORG images reconstructed with a duty cycle of 50 %, 35 %, and 20 %, the absolute SUV_{mean} increased to 11.2 ± 6.5 , 11.4 ± 6.6 , and 11.5 ± 6.6 , respectively. In addition to the observed differences in SUV_{mean} and volume, some lesions also demonstrated marked changes in morphology when respiratory gating was performed. These effects of respiratory gating are readily shown in Fig. 3 that depict non-gated and ORG PET images of a patient with a non-small cell lung cancer (NSCLC) lesion in the left lower lobe.

A considerable difference in magnitude of the effect of ORG on lesion volume and on SUV_{mean} for the different anatomical locations was observed. The mean increase in lesion SUV_{mean} and reduction in volume as a function of the percentage duty cycle and anatomical location are summarized in Tables 2 and 3, respectively. The changes in SUV_{mean} and in volume were largest for lesions in the middle and lower lobes. For lesions located in the middle and lower lobes, statistically significant increases in SUV_{mean} were observed for duty cycles of 50 %, 35 % and 20 %, whereas statistically significant volume reductions were observed for duty cycles of 35 % and 20 %. However, for lesions located in the upper lobes and centrally located lesions, the effect of ORG was smaller. For centrally located lesions, a statistically significant SUV_{mean} increase was observed for duty cycles of 50 %, 35 % and 20 %, whereas a statistically significant volume reduction was only observed for a duty cycle of 20 %. For lesions located in the upper lobes, a statistically significant increase in lesion SUV_{mean} and reduction in volume was observed only for duty cycles of 20 %. Figure 4 readily depicts such an anatomical dependency of the effects of ORG in a single patient with two NSCLC lesions, one located in the left lower lobe and one in the left lung hilum.

In this patient, the large NSCLC lesion located in the left lung hilum (depicted in Fig. 3c and d) exhibits invasive growth into the left main bronchus, causing a post obstructive atelectasis of the left lower lobe in which a second NSCLC lesion is located. For the lesion in the left lung hilum, the SUV_{mean} increase in the ORG image was 5.3 % when compared to the non-gated image, and a concomitant decrease in volume of 1.9 % was observed. The effects of ORG on the

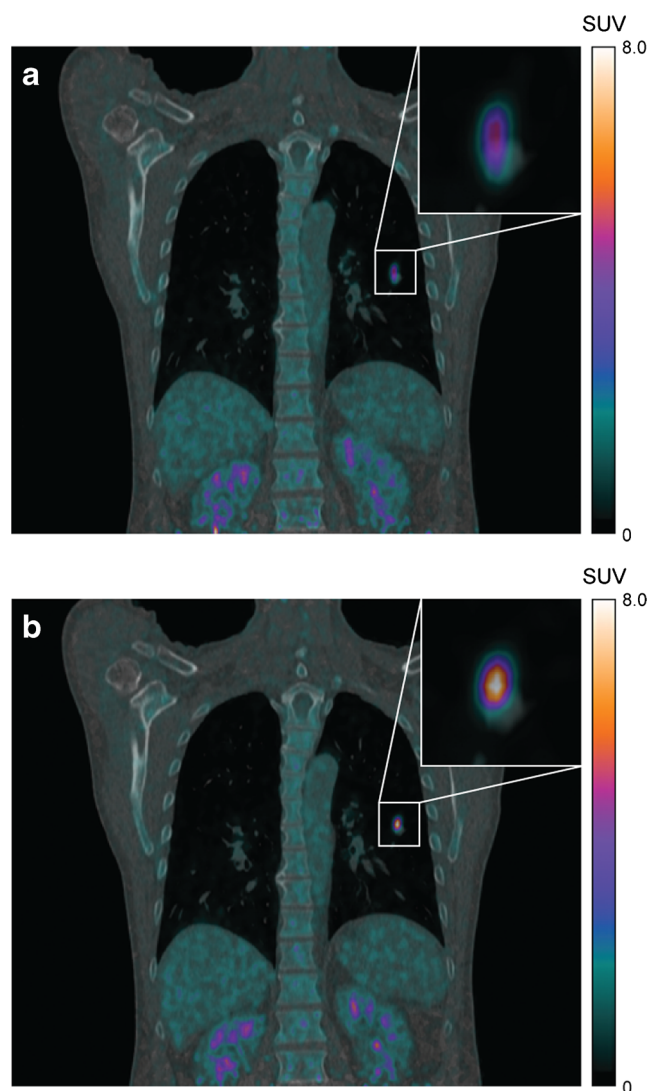


Fig. 3 Coronal non-gated and ORG PET images of a patient with a NSCLC lesion in the left lower lobe fused with LDCT images. **a)** Non-gated PET image fused with a LDCT image, **b)** ORG PET image reconstructed with a 35 % duty cycle fused with a LDCT image. The PET and CT images are displayed with equal window level settings. In addition to a different morphological appearance of the lesion between the non-gated and ORG PET images, there is a considerable increase in SUV_{mean} of 69.5 % and a decrease in volume of 80.2 %. SUV =standardized uptake value

lesion in the left lower lobe were considerably larger, showing a SUV_{mean} increase of 31.9 % and a concomitant volume decrease of 23.0 %. Analysis revealed no correlation between lesion size, as determined on the non-gated images, and relative increase in SUV_{mean} . The Spearman correlation coefficient ‘ ρ ’, describing the relation between lesion size and SUV_{mean} increase, was -0.129, -0.169, and -0.212 for duty cycles of 50 %, 35 %, and 20 %, respectively.

The values for the coefficients of variation revealed that the amount of image noise is increased when lower percentages of the duty cycle are used for image reconstruction. The mean coefficients of variation of the VOIs located in the

Table 2 Relative SUV_{mean} increase of lesions in the ORG images compared to the non-gated images for different anatomical locations and percentages duty cycle.

Anatomical location	Duty Cycle [%]		
	50	35	20
Upper lobes (n=28)	3.6±11.6 % (p=0.8)	5.0±12.2 % (p=0.2)	6.9±13.5 % (p=0.02) *
Middle and lower lobes (n=26)	12.3±15.7 % (p<0.0001) *	13.7±16.8 % (p<0.0001) *	15.5±17.7 % (p<0.0001) *
Central (n=29)	3.2±5.8 % (p=0.04) *	4.2±7.3 % (p=0.01) *	5.8±7.7 % (p<0.0001) *
All locations (n=83)	6.2±12.2 % (p<0.0001) *	7.4±13.3 % (p<0.0001) *	9.2±14.0 % (p<0.0001) *

Data are reported as mean ±standard deviation
* Statistically significant

contralateral lung parenchyma of the 66 patients are summarized in Table 4. Although selection of a higher percentage duty cycle for image reconstruction reduces the amount of image noise, this will inevitably result in calculation of a wider amplitude range and a larger residual motion component residing in the reconstructed images. The mean width of the amplitude range for duty cycles of 50 %, 35 %, and 20 %, is summarized in Table 5.

Discussion

The clinical role of FDG PET for management of patients with primary lung cancer is increasingly being recognized [20, 25, 26]. Several authors report a correlation between changes in lesion glucose metabolism in subsequent PET imaging and treatment response [10, 17, 27]. However, respiratory motion can introduce random errors during image quantification in PET and, if uncorrected, may hinder adequate patient management. Reducing inaccuracies regarding quantification of lesion volume and radiotracer uptake may improve monitoring treatment response in early stages of cancer therapy, facilitating clinical decision making by switching to a different treatment regimen, thereby avoiding administration of several cycles of ineffective anti-cancer treatment [21]. Furthermore, with the increasing tendency to incorporate functional information provided by PET imaging into radiation treatment planning schemes, correction of PET images for respiratory motion artefacts may enable the possibility to employ a more individually tailored radiation therapy [1, 3, 24]. Particularly, the reduction in target volume could be used to perform

radiation dose escalation on the lesion whilst limiting the dose to organs at risk.

Traditionally, techniques that rely on the use of a respiratory surrogate signal in order to perform respiratory gating can be characterized as either phase-based or amplitude-based. Phased-based respiratory gating methods perform sorting of list-mode data by dividing each respiratory cycle into a fixed number of respiratory gates of equal duration. Respiratory gating of PET data is then performed by using PET data collected in a specific gate for image reconstruction. However, these methods are sensitive to the emergence irregular breathing patterns during image acquisition. These irregular patterns hinder appropriate detection of respiratory peaks in the signal resulting in rejection of respiratory cycles that can be used for gating. Discarding PET data can considerably reduce diagnostic quality of the PET images due to increased amounts of image noise. Several authors reported that amplitude-based approaches are more robust in the presence of irregular breathing patterns when compared to phase-based gating approaches [7, 9, 18]. However, most of these algorithms do not take the characteristics of the respiratory signal into consideration. The advantage of the ORG algorithm is that it finds the optimal amplitude range for the specified duty cycle. Calculation of the optimal amplitude range is achieved by searching throughout the entire respiratory signal of the gated bed positions the smallest amplitude range, which still contains the specified amount of PET data. The ORG algorithm, therefore, makes optimal use of specific characteristics of the respiratory signal, such as plateau phases, to define an optimal amplitude range while maintaining image quality. Selection of the duty cycle permits the user to control the amount of noise and residual motion in the image.

Table 3 Relative volume decrease of lesions in the ORG images compared to the non-gated images for different anatomical locations and percentages duty cycle

Anatomical location	Duty Cycle [%]		
	50	35	20
Upper lobes (n=28)	3.3±17.5 % (p=1)	5.8±19.9 % (p=1)	8.2±23.3 % (p=0.03) *
Middle and lower lobes (n=26)	13.3±24.9 % (p=0.07)	14.8±23.3 % (p=0.006) *	17.7±21.0 % (p<0.0001) *
Central (n=29)	4.7±15.1 % (p=1)	5.3±13.1 % (p=0.4)	8.6±14.9 % (p=0.02) *
All locations (n=83)	6.9±19.6 % (p=0.02) *	8.5±19.3 % (p<0.0001) *	11.3±20.2 % (p<0.0001) *

Data are reported as mean ±standard deviation
* Statistically significant

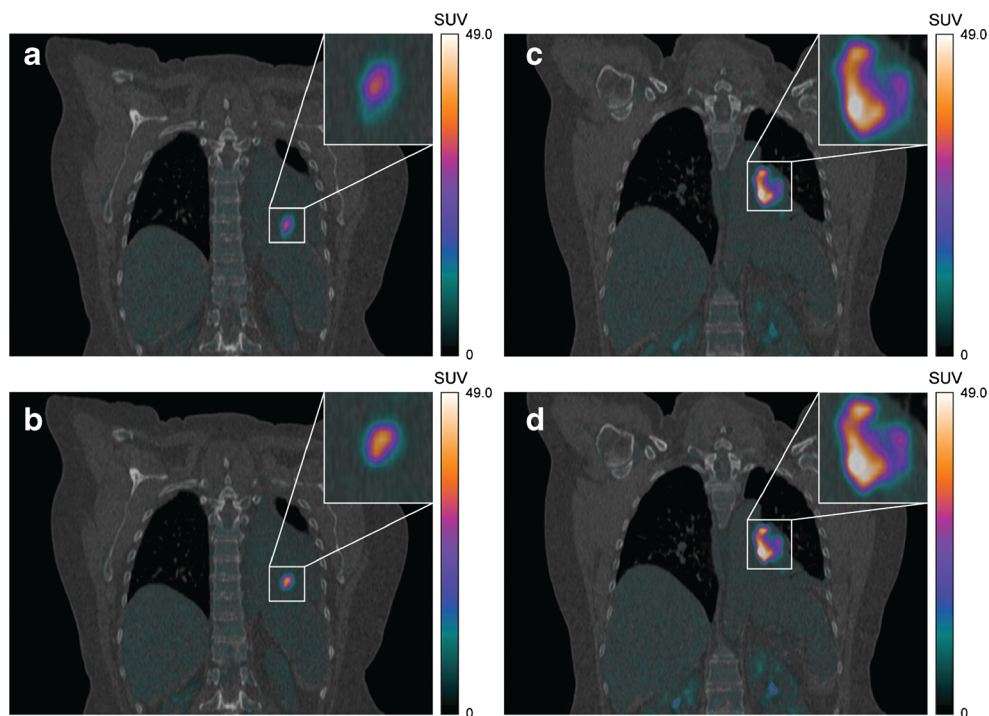


Fig. 4 Non-gated and ORG PET images fused with LDCT images of a patient with NSCLC lesions in the left lower lobe and lung hilum. **a)** Non-gated PET image fused with a LDCT image depicting a lesion in the left lower lobe, **b)** ORG PET image, reconstructed with a duty cycle of 35 %, fused with a LDCT image of a lesion in the left lower lobe, **c)** Non-gated PET image fused with a LDCT image depicting a lesion in the left lung hilum, **d)** ORG PET image, reconstructed with a duty cycle of 35 %, fused with a LDCT image of a lesion in the left lung hilum. The PET and

CT images are displayed using equal window level settings. In this patient, the anatomical dependency of the effects of ORG is clearly demonstrated. For the lesion in the left lung hilum, the SUV_{mean} increase in the ORG image was 5.3 % while a concomitant decrease in volume of 1.9 % was observed. A considerable larger increase in SUV_{mean} of 31.9 % and decrease in volume of 23.0 % was observed for the lesion in the left lower lung lobe. SUV =standardized uptake value

The results of this study show that respiratory gating with HD-Chest considerably affects quantification of lesion volume and FDG-uptake during PET imaging of the thorax. The effects are dependent on the anatomical location of the lesion and percentage duty cycle used for image reconstruction. In general, lesions in the middle and lower lung lobes demonstrate a considerable increase in SUV_{mean} and reduction in volume when ORG is performed. However, the effect of ORG on lesions located centrally and in the upper lobes is more heterogeneous. The heterogeneity of the observed effects can be explained by the classification of the lesions into three main

anatomical groups used during this study. The exact location of a lesion, as well as the extension of lesion growth (e.g., attachment to other anatomical structures), determines the displacement of the lesion during the patient's respiratory cycle. For the upper lung lobes, lesions in the apical segments usually experienced limited displacement during the respiratory cycle, whilst lesions in the inferior segments demonstrated more substantial displacement. The same differences were observed for centrally located lesions, where lesions located in the periphery of the lung hilum demonstrated larger increases in SUV_{mean} and reduction in volume whereas almost no effects were observed for mediastinal and subcarinal lesions.

In this study, we examined a representative patient population from our fast-track outpatient diagnostic program. However, a number of these patients presented with additional

Table 4 Mean coefficient of variation for the VOIs in the contralateral lung parenchyma for duty cycles of 50 %, 35 %, and 20 %. The non-gated images were reconstructed with 360 s (100 %) and 126 s (35 %) of the acquired true coincidences per bed position

Percentage duty cycle [%]	Non-gated 50	Non-gated 35	20
True coincidences [s]	360	180	126
Coefficient of variation [%]	26.1±6.4	30.1±8.0	31.8±5.6
		32.8±6.4	39.4±7.5

Data are reported as mean±standard deviation

Table 5 Mean width of the amplitude range used for ORG for duty cycles of 50 %, 35 %, and 20 %. The amplitude range is calculated by subtracting the value for the lower amplitude limit from that of the upper amplitude limit

Percentage duty cycle [%]	50	35	20
Width of Amplitude range [%]	20.9±5.9	12.9±5.1	7.3±2.4

Data are reported as mean±standard deviation

pulmonary diseases such as lung emphysema and fibrosis. Particularly in patients with severe lung emphysema, thoracic wall excursions and displacement of anatomical structures can be reduced due to hyperinflation. In this patient population, approximately one third of the patients had radiological evidence of mild lung emphysema. However, no considerable reduction in breathing excursions on the acquired respiratory signals were observed as compared to the patients without emphysema. Furthermore, there was no correlation other than anatomical location between the presence of lung emphysema and observed increases in SUV_{mean} and decreases in volume.

It should be mentioned that the ORG algorithm deals with PET data only. Since the CT examinations have been performed without respiratory gating and without breathing instructions, a spatial mismatch between the PET and CT images can exist, particularly for structures which exhibit a large displacement during the respiratory cycle. Spatial mismatch between the PET and CT datasets may result in inappropriate attenuation correction and subsequent inaccuracies in quantification of the PET images. Several authors report strategies to improve spatial match between PET and CT images [16, 23]. These strategies include the use of breathing instructions, and respiratory triggered or gated CT acquisitions using the same respiratory signal as during PET gating. Optimizing the spatial matching of PET and attenuation CT images in combination with the ORG algorithm will be the subject of future study.

Respiratory gating with HD·Chest permits convenient integration of respiratory gating of multiple bed positions in a whole body PET imaging protocol and can easily be integrated in a routine clinical PET workflow. Furthermore, the advantages of modern PET reconstruction algorithms, including the incorporation of TOF and a spatially varying PSF, can be used in image reconstruction of respiratory gated PET data. The results of this study suggest that respiratory gating could influence clinical PET imaging with respect to therapy response monitoring and radiation treatment planning.

Conclusion

ORG with HD·Chest markedly affects quantification of lesion volume and FDG-uptake in PET imaging of the thorax, particularly for lesions located in the middle and lower lung lobes. The results of this study show that the magnitude of the effects is dependent on the anatomical location of the lesion and the percentage duty cycle used for image reconstruction. These results imply that ORG could influence clinical PET imaging with respect to therapy response monitoring and radiation treatment planning.

Acknowledgments The scientific guarantor of this publication is dr. E.P. Visser, Department of Radiology and Nuclear Medicine, Radboud university medical center, Nijmegen, The Netherlands. The authors of

this manuscript declare no relationships with any companies, whose products or services may be related to the subject matter of the article. This study has received funding by Siemens Healthcare, The Hague, The Netherlands. This study was supported by an educational grant from Siemens Healthcare, The Hague, The Netherlands. The authors would like to thank James Hamill (Siemens) for scientific input. No complex statistical methods were necessary for this paper. Institutional Review Board approval was obtained. Written informed consent was waived by the Institutional Review Board.

Methodology Retrospective, experimental, performed at one institution.

References

1. Bentzen SM, Gregoire V (2011) Molecular Imaging–Based Dose Painting: A Novel Paradigm for Radiation Therapy Prescription. *Semin Radiat Oncol* 2:101–110
2. Berghmans T, Dusart M, Paesmans M et al (2008) Primary Tumor Standardized Uptake Value (SUV_{max}) Measured on Fluorodeoxyglucose Positron Emission Tomography (FDG-PET) is of Prognostic Value for Survival in Non-small Cell Lung Cancer (NSCLC): A Systematic Review and Meta-Analysis (MA) by the European Lung Cancer Working Party for the IASLC Lung Cancer Staging Project. *J Thorac Oncol* 1:6–12
3. Bettinardi V, Picchio M, Di Muzio N, Gilardi MC (2012) Motion Management in Positron Emission Tomography/Computed Tomography for Radiation Treatment Planning. *Semin Nucl Med* 5: 289–307
4. Bomanji JB, Costa DC, Ell PJ (2001) Clinical role of positron emission tomography in oncology. *Lancet Oncol* 3:157–164
5. Callahan J, Binns D, Dunn L, Kron T (2011) Motion effects on SUV and lesion volume in 3D and 4D PET scanning. *Australas Phys Eng Sci Med* 4:489–495
6. Carney JPJ, Townsend DW, Rappoport V, Bendriem B (2006) Method for transforming CT images for attenuation correction in PET/CT imaging. *Med Phys* 4:976–983
7. Chang G, Chang T, Pan T, Clark JW, Mawlawi OR (2010) Implementation of an Automated Respiratory Amplitude Gating Technique for PET/CT: Clinical Evaluation. *J Nucl Med* 1:16–24
8. Chen HHW, Chiu N-T, Su W-C, Guo H-R, Lee B-F (2012) Prognostic Value of Whole-Body Total Lesion Glycolysis at Pretreatment FDG PET/CT in Non-Small Cell Lung Cancer. *Radiology* 2:559–566
9. Dawood M, Buther F, Lang N, Schober O, Schafers KP (2007) Respiratory gating in positron emission tomography: A quantitative comparison of different gating schemes. *Med Phys* 7:3067–3076
10. de Geus-Oei L-F, van der Heijden HFM, Visser EP et al (2007) Chemotherapy Response Evaluation with 18 F-FDG PET in Patients with Non-Small Cell Lung Cancer. *J Nucl Med* 10:1592–1598
11. de Geus-Oei LF, van Laarhoven HWM, Visser EP et al (2008) Chemotherapy response evaluation with FDG–PET in patients with colorectal cancer. *Ann Oncol* 2:348–352
12. Dose Schwarz J, Bader M, Jenicke L, Hemminger G, Jänicke F, Avril N (2005) Early Prediction of Response to Chemotherapy in Metastatic Breast Cancer Using Sequential 18 F-FDG PET. *J Nucl Med* 7:1144–1150
13. Elmpt W, Hamill J, Jones J, Ruyscher D, Lambin P, Öllers M (2011) Optimal gating compared to 3D and 4D PET reconstruction for characterization of lung tumours. *Eur J Nucl Med Mol Imaging* 5:843–855
14. Erdi YE, Malawi O, Larson SM et al (1997) Segmentation of Lung Lesion Volume by Adaptive Positron Emission Tomography Image Thresholding. *Cancer* 12:2505–2509

15. Fletcher JW, Djulbegovic B, Soares HP et al (2008) Recommendations on the Use of 18 F-FDG PET in Oncology. *J Nucl Med* 3:480–508
16. Goerres G, Kamel E, Heidelberg T-N, Schwitter M, Burger C, von Schulthess G (2002) PET-CT image co-registration in the thorax: influence of respiration. *Eur J Nucl Med Mol Imaging* 3:351–360
17. Hoekstra CJ, Stroobants SG, Smit EF et al (2005) Prognostic Relevance of Response Evaluation Using [18 F]-2-Fluoro-2-Deoxy-D-Glucose Positron Emission Tomography in Patients With Locally Advanced Non-Small-Cell Lung Cancer. *J Clin Oncol* 33: 8362–8370
18. Jani SS, Robinson CG, Dahlbom M et al (2013) A Comparison of Amplitude-Based and Phase-Based Positron Emission Tomography Gating Algorithms for Segmentation of Internal Target Volumes of Tumors Subject to Respiratory Motion. *Int J Radiat Oncol Biol Phys* 3:562–569
19. Korreman SS (2012) Motion in radiotherapy: photon therapy. *Phys Med Biol* 23:R161–R191
20. Mac Manus MP, Hicks RJ, Matthews JP et al (2003) Positron Emission Tomography Is Superior to Computed Tomography Scanning for Response-Assessment After Radical Radiotherapy or Chemoradiotherapy in Patients With Non-Small-Cell Lung Cancer. *J Clin Oncol* 7:1285–1292
21. Mikhaeel NG, Hutchings M, Fields PA, O'Doherty MJ, Timothy AR (2005) FDG-PET after two to three cycles of chemotherapy predicts progression-free and overall survival in high-grade non-Hodgkin lymphoma. *Ann Oncol* 9:1514–1523
22. Nehmeh SA, Erdi YE (2008) Respiratory Motion in Positron Emission Tomography/Computed Tomography: A Review. *Semin Nucl Med* 3:167–176
23. Nehmeh SA, Erdi YE, Pan T et al (2004) Four-dimensional (4D) PET/CT imaging of the thorax. *Med Phys* 12:3179–3186
24. Nestle U, Kremp S, Grosu A-L (2006) Practical integration of [18 F]-FDG-PET and PET-CT in the planning of radiotherapy for non-small cell lung cancer (NSCLC): The technical basis, ICRU-target volumes, problems, perspectives. *Radiother Oncol : J Eur Soc Ther Radiol Oncol* 2:209–225
25. Shankar LK, Hoffman JM, Bacharach S et al (2006) Consensus Recommendations for the Use of 18 F-FDG PET as an Indicator of Therapeutic Response in Patients in National Cancer Institute Trials. *J Nucl Med* 6:1059–1066
26. Weber WA (2005) Use of PET for Monitoring Cancer Therapy and for Predicting Outcome. *J Nucl Med* 6:983–995
27. Weber WA, Petersen V, Schmidt B et al (2003) Positron Emission Tomography in Non-Small-Cell Lung Cancer: Prediction of Response to Chemotherapy by Quantitative Assessment of Glucose Use. *J Clin Oncol* 14:2651–2657
28. Zaizen Y, Azuma K, Kurata S et al (2012) Prognostic significance of total lesion glycolysis in patients with advanced non-small cell lung cancer receiving chemotherapy. *Eur J Radiol* 12:4179–4184